

# Reduced Complexity Resource Allocation For Frequency Domain Non-orthogonal Multiple Access

Satoshi Denno, Taichi Yamagami, and Yafei Hou

Graduate School of Natural Science and Technology, Okayama University

3-1-1 Tsushima-naka, Kita Okayama, 700-8530 Japan

denno@okayama-u.ac.jp

**Abstract**—This paper proposes low complexity resource allocation in frequency domain non-orthogonal multiple access where many devices access with a base station. The number of the devices is assumed to be more than that of the resource for network capacity enhancement, which is demanded in massive machine type communications (mMTC). This paper proposes two types of resource allocation techniques, which are named as “CGVS” and “LLRVS”, all of which are based on the MIN-MAX approach. CGVS seeks for nicer resource allocation with only channel gains, while LLRVS applies the message passing algorithm (MPA) for better resource allocation. The proposed resource allocation techniques are evaluated by computer simulation in frequency domain non-orthogonal multiple access. Whereas LLRVS achieves only 0.1dB better performance than CGVS in the multiple access with the overloading ratio of 1.5 at the BER of  $10^{-4}$ , CGVS can be implemented with  $10^{-5}$  smaller computational complexity than LLRVS. CGVS attains a gain of about 10dB at the BER of  $10^{-4}$  in the multiple access with the overloading ratio of 2.0. The complexity of CGVS is  $10^{-16}$  as small as the conventional technique.

**Index Terms**—Non-orthogonal access, low complexity, message passing algorithm, subcarrier allocation

## I. INTRODUCTION

Machine-type communications (MTC) have been identified as a part of the fifth generation mobile communication system and the beyond 5th generation system for the society with Internet of things (IoT). The society with the IoT needs a lot of sensor devices with wireless communication functionality, which are going to be scattered around us. Massive connectivity is demanded for the connection with those devices when the number of those devices grows extremely high. In a word, network capacity has to be increased for such massive MTC (mMTC), though amount of data sent by a device might not be huge. Many techniques have been proposed for enhancement of the wireless network capacity. For instance, multi-user multiple input multiple output (MU-MIMO) [1] and orthogonal frequency division multiple access (OFDMA) [2], that are classified into orthogonal multiple access, have been investigated. Non-orthogonal multiple access also has been considered, because non-orthogonal multiple access potentially achieves higher capacity than orthogonal multiple access. Non-orthogonal multiple access (NOMA) [3]–[9], low-density signature (LDS) [10], [11], and sparse code multiple access (SCMA) [12], [13] have been proposed as non-orthogonal multiple access techniques. Adaptive resource allocation has been proposed for non-orthogonal multiple access based on

low density signature [14]. Although the adaptive resource allocation improves the transmission performance, the allocation technique executes the message passing algorithm (MPA) [15], [16] for all the subcarrier allocation patterns to find the best resource allocation at the transmitter, which results in prohibitive high computational complexity.

In this paper, we propose low complexity resource allocation in frequency domain non-orthogonal multiple access where many devices access with a base station. Whereas our proposed techniques search better resource allocation based on the MIN-MAX approach, our proposed techniques can be classified into two types. One of them seeks for nicer resource allocation with only channel gains. The other applies the message passing algorithm (MPA) only for the nice candidates of resource allocation, while the conventional technique executes the MPA for all the resource allocation patterns. The performance of those proposed techniques are evaluated by computer simulations. The proposed techniques achieve as near optimum performance as the conventional technique. However, the proposed techniques can be implemented with much less computational complexity than the conventional technique.

Throughout the paper,  $j$ , and  $c^*$  represent the imaginary unit, and complex conjugate of a complex number  $c$ . Superscript  $T$  and  $H$  indicate transpose and Hermitian transpose of a matrix or a vector, respectively. In addition,  $\text{diag}[\mathbf{V}]$ ,  $\mathbf{A}_l$ ,  $\mathbf{A}_{\{k\}}$  and  $\mathbf{A}_{k,l}$  indicate a diagonal matrix with a vector  $\mathbf{V}$  in the diagonal position, an  $l$ th column vector, a  $k$ th row vector, and a  $(k, l)$  element of a matrix  $\mathbf{A}$ , respectively.

## II. SYSTEM MODEL

We assume that a user owns  $L$  IoT devices for collecting information measured with the sensors on the devices, and one resource block is allocated to the user. In other words, the user communicates with those IoT devices through wireless communication within the allocated resource block. The number of the devices is possibly increasing regardless of the resource. The transmitters on the IoT devices are assumed to have always some information to send, which forces all the IoT devices to send their packet simultaneously for the receiver on the base station. Only one antenna is installed on every IoT device and the base station. The available frequency resources are defined using a set  $\mathbf{B}_F = \{b(0), b(1), \dots, b(N_s - 1)\}$  where  $N_s \in \mathbb{N}$  and  $b(l) \in \mathbb{R}$  denote the number of the

subcarriers in a resource block and  $l$ th subcarrier number in the resource block. Let  $N_F \in \mathbb{N}$  and  $n \in \mathbb{N}$  represent the number of the discrete Fourier transform (DFT) points and an iteration stage number defined afterwards, the  $l$ th device transmits a signal vector  $\mathbf{S}_l^{(n)} \in \mathbb{C}^{N_F}$  with a partial discrete Fourier transform matrix (PDFT)  $\dot{\mathbf{F}} \in \mathbb{C}^{N_s \times N_F}$  as,

$$\mathbf{S}_l^{(n)} = \dot{\mathbf{F}} \mathbf{H} \mathbf{X}^{(n)}(l). \quad (1)$$

In (1),  $\mathbf{X}^{(n)}(l) \in \mathbb{C}^{N_s}$  represents a modulation signal vector sent from the  $l$ th device. Let  $\dot{\mathbf{F}}_{p,q} \in \mathbb{C}$  represent a  $(p, q)$  element of the PDFT matrix, the PDF matrix  $\dot{\mathbf{F}}$  is defined as,

$$\dot{\mathbf{F}}_{p,q} = \frac{1}{\sqrt{N_F}} e^{-j \frac{2\pi b(p-1)(q-1)}{N_F}}. \quad (2)$$

Though the device transmits the signals in multiple frequency resources, i.e. subcarriers, the same modulation signal  $x(l) \in \mathbb{C}$  is sent in the subcarriers.

$$\mathbf{X}^{(n)}(l) = \mathbf{C}_l^{(n)} x(l), \quad (3)$$

In (3),  $\mathbf{C}_l^{(n)} \in \mathbb{R}^{N_s}$  represents a subcarrier allocation vector for the  $l$ th device, which is defined as  $\mathbf{C}_l^{(n)} = [c_{l,0}^{(n)} \cdots c_{l,N_s-1}^{(n)}]^T$  where  $c_{l,i-1}^{(n)} \in \mathbb{R}$  indicates the  $i$ th element of the vector  $\mathbf{C}_l^{(n)}$ . The element defines availability of the subcarrier for the device to send the signals, which is defined as follows.

$$c_{l,i-1}^{(n)} = \begin{cases} 1 & (i \text{ th subcarrier is available}) \\ 0 & (i \text{ th subcarrier is not available}) \end{cases} \quad (4)$$

As is shown in (3) and (4), the device actually only transmits the same packet in the  $M$  subcarriers where  $M$  indicates the number of the subcarriers allocated to an IoT device. Let  $\mathbf{C}^{(n)} \in \mathbb{C}^{N_s \times L}$  denote a subcarrier allocation matrix, the matrix is defined as  $\mathbf{C}^{(n)} = [\mathbf{C}_1^{(n)} \cdots \mathbf{C}_L^{(n)}]$ .

All the devices simultaneously send their packets for the base station after the cyclic prefixes are added to those signals. The base station receives those transmission signals that have passed through multipath fading channels, where the path length is less than the cyclic prefix length. Let  $\mathbf{H}_l \in \mathbb{C}^{N_F \times N_F}$  denote a channel matrix between the  $l$ th device and the base station, a received signal vector  $\mathbf{Y} \in \mathbb{C}^{N_F}$  in the time domain can be written as,

$$\mathbf{Y} = \sum_{l=1}^L \mathbf{H}_l \mathbf{S}_l^{(n)} + \mathbf{N}. \quad (5)$$

In (5),  $\mathbf{N} \in \mathbb{C}^{N_F}$  represents an additive white Gaussian noise (AWGN) vector. As is shown in (5), the received signal is superposition of the transmission signals from the  $L$  devices. The received signal vector in the time domain is transformed into the frequency domain as,

$$\begin{aligned} \dot{\mathbf{Y}} &= \dot{\mathbf{F}} \mathbf{Y} = \sum_{l=1}^L \dot{\mathbf{F}} \mathbf{H}_l \mathbf{S}_l^{(n)} + \dot{\mathbf{F}} \mathbf{N} \\ &= \bar{\mathbf{\Gamma}}^{(n)} \mathbf{X} + \dot{\mathbf{F}} \mathbf{N} \end{aligned} \quad (6)$$

In the above equation,  $\dot{\mathbf{Y}} \in \mathbb{C}^{N_s}$  and  $\mathbf{X}$  denote a received signal vector in the frequency domain and a transmission signal vector containing all the devices' transmission signals defined as  $\mathbf{X} = (x(1) \cdots x(L))^T$ . In addition,  $\bar{\mathbf{\Gamma}}^{(n)} \in \mathbb{C}^{N_s \times L}$  represents an equivalent channel matrix defined as,

$$\bar{\mathbf{\Gamma}}^{(n)} = [\mathbf{\Gamma}(1) \mathbf{C}_1^{(n)} \cdots \mathbf{\Gamma}(L) \mathbf{C}_L^{(n)}]. \quad (7)$$

In (7),  $\mathbf{\Gamma}(l) \in \mathbb{C}^{N_s \times N_s}$  denotes a diagonal matrix with the frequency responses between the  $l$ th device and the base station in the diagonal positions, which is expressed as follows.

$$\mathbf{\Gamma}(l) = \text{diag}[\gamma_l(0) \gamma_l(1) \cdots \gamma_l(N_s - 1)] \quad (8)$$

In (8),  $\gamma_l(m)$  represents a frequency response in the  $m$ th subcarrier between the  $l$ th device and the base station, which is defined as,

$$\gamma_l(m) = \sum_{p=0}^{L_p-1} h_l(p) \exp\left(-j2\pi \frac{mp}{N_F}\right), \quad (9)$$

where  $L_p \in \mathbb{N}$  and  $h_l(p) \in \mathbb{C}$  denote the number of the paths in the multipath fading channel and a complex path gain of the  $p$ th path in the channel between the  $l$ th IoT device and the base station.

Even when superposition of the transmission signals sent from the  $L$  terminals is received at the receiver on the base station, if the equivalent channel matrix is sparse, a low complexity detector based on the MPA can be applied, which achieves almost the same performance to the maximum likelihood estimation.

For enhancing transmission performance, the adaptive resource allocation has been proposed [14]. However, it needs the prohibitive high complexity that grows exponentially with the number of the terminals  $L$ ; the MPA is executed  $Q^L \binom{L}{1}$  times, where  $Q$  represents cardinality of the modulation, because the exhaustive search is applied.

We propose low complexity resource allocation algorithm in the following section.

### III. REDUCED COMPLEXITY RESOURCE ALLOCATION

Even when a detector based on the MPA is applied at the receiver, the performance is dependent on the channel matrix in the system. This means that the detection performance could be estimated through analysis of the channel matrix in the system with the frequency domain non-orthogonal multiple access. This section proposes low complexity resource allocation based on analysis of the channel matrix.

#### A. Least Channel Gain Maximization With Channel Vector Swapping

This section applies vector swapping to the subcarrier allocation matrix, with which resource allocation can be implemented. The vector swapping is iterated until better resource allocation is found in the proposed technique. Let  $\bar{\mathbf{\Gamma}}^{(n)}$  denote an equivalent channel matrix at the  $n$ th iteration stage, first of

all, the position of the minimum channel gain  $\bar{\Gamma}_{k_n, l_n}^{(n)} \in \mathbb{C}$  in the equivalent channel matrix is searched as,

$$(k_n, l_n) = \arg \min_{(k, l) \in B^{(n)}} \left[ \left| \bar{\Gamma}_{k, l}^{(n)} \right| \right]. \quad (10)$$

$B^{(n)}$  in (10) represents a set containing the positions of the non-zero elements in the matrix  $\bar{\Gamma}^{(n)}$ , which is defined as  $B^{(n)} = \{(k, l) | \bar{\Gamma}_{k, l}^{(n)} \neq 0\}$ . For the vector swapping, a permutation matrix  $\mathbf{J}(l_1 \leftrightarrow l_2) \in \mathbb{N}^{L \times L}$  is introduced to swap  $l_1$ th column and  $l_2$ th column as follows.

$$\mathbf{J}(l_1 \leftrightarrow l_2) = \begin{pmatrix} & (l_1) & & (l_2) \\ 1 & \vdots & & \vdots \\ & \ddots & & \\ & & 0 & \dots & 1 \\ & \vdots & & \vdots & \\ & 1 & \dots & 0 & \\ & & & & \ddots \\ & & & & & 1 \end{pmatrix} \quad (11)$$

A candidate subcarrier allocation matrix  $\mathbf{C}^{[r_n]} \in \mathbb{C}^{N_s \times L}$  and a candidate equivalent channel matrix  $\bar{\Gamma}^{[r_n]} \in \mathbb{C}^{N_s \times L}$  are obtained with the permutation matrix as follows.

$$\mathbf{C}^{[r_n]} = \mathbf{C}^{(n)} \mathbf{J}(l_n \leftrightarrow r_n) \quad (12)$$

$$\bar{\Gamma}^{[r_n]} = [\bar{\Gamma}(1) \mathbf{C}_1^{[r_n]} \dots \bar{\Gamma}(L) \mathbf{C}_L^{[r_n]}] \quad (13)$$

In (12) and (13),  $r_n \in \mathbb{N}$  represents a column index different from  $l_n$ . Let  $B_l^{[r_n]}$  denote a set containing the positions of the nonzero elements in the  $l$ th column vector of the matrix  $\bar{\Gamma}^{[r_n]}$ , the set is defined as  $B_l^{[r_n]} = \{k | \bar{\Gamma}_{k, l}^{[r_n]} \neq 0\}$ . The position of the minimum non-zero element in the  $l_n$ th and  $r_n$ th column vectors is searched as,

$$(k^{[r_n]}, l^{[r_n]}) = \arg \min \left[ \left| \bar{\Gamma}_{k_1, l_n}^{[r_n]} \right|, \left| \bar{\Gamma}_{k_2, r_n}^{[r_n]} \right| \right] \quad (14)$$

$$(k_1, l_n) \in B_{l_n}^{[r_n]}$$

$$(k_2, r_n) \in B_{r_n}^{[r_n]}$$

Since the  $l_n$ th column can be swapped with all the columns except for  $l_n$ th column, we find the best column that provides the biggest value  $\bar{\Gamma}_{k^{[r_n]}, l^{[r_n]}}^{[r_n]}$ , which is written as follows.

$$\bar{r}_n = \arg \max_{r_n} \left[ \bar{\Gamma}_{k^{[r_n]}, l^{[r_n]}}^{[r_n]} \right] \quad (15)$$

$\bar{r}_n \in \mathbb{N}$  represents a column index that makes the permutation provide the biggest value  $\bar{\Gamma}_{k^{[r_n]}, l^{[r_n]}}^{[r_n]}$  in the indexes  $r_n = 1 \dots L$ . The best candidate subcarrier allocation matrix  $\mathbf{C}^{(n+1/n)} \in \mathbb{C}^{N_s \times L}$  can be obtained with the column index  $\bar{r}_n$  as follows.

$$\mathbf{C}^{(n+1/n)} = \mathbf{C}^{(n)} \mathbf{J}(l_n \leftrightarrow \bar{r}_n) \quad (16)$$

The above signal processing is depicted by Fig. 1 where the equivalent channel matrices with  $N_s = 4$ ,  $M = 2$ , and  $L = 6$  are shown.  $\gamma_l(k)$  is equal to a  $(k, l)$  element of the channel matrix  $\bar{\Gamma}^{(n)}$ , i.e.,  $\gamma_l(k) = \bar{\Gamma}_{k, l}^{(n)}$ . The channel gain  $\gamma_4(2)$  is

assumed to be the smallest in the upper matrix in the figure. The subcarriers allocated to the 4th device are attempted to be reallocated to the other device<sup>1</sup>. If the subcarriers are swapped with those to the 3rd device, for example, the lower equivalent channel matrix will be obtained. The smallest gain in the subcarriers for the 3rd and 4th devices is searched, which is implemented in (14). The above attempt is repeated with all the possible columns, and the smallest gains given by all the attempts are compared. When the attempt with the  $\bar{r}_n$ th device attains the largest gain, which is done in (15), the subcarriers allocated to the 4th device are swapped with those of the  $\bar{r}_n$ th device. The permutation matrix corresponding to the swap is selected for the best candidate subcarrier allocation matrix as shown in (16).

The subcarrier allocation matrix  $\mathbf{C}^{(n)}$  is updated as,

$$\mathbf{C}^{(n+1)} = \begin{cases} \mathbf{C}^{(n+1/n)} & \left| \bar{\Gamma}_{k_n, l_n}^{(n)} \right| < \left| \bar{\Gamma}_{k^{[\bar{r}_n]}, l^{[\bar{r}_n]}}^{[\bar{r}_n]} \right| \\ \mathbf{C}^{(n)} & \text{otherwise} \end{cases} \quad (17)$$

This means that the subcarrier allocation matrix is updated only if the update of the subcarrier allocation matrix makes the absolute value  $\left| \bar{\Gamma}_{k^{[\bar{r}_n]}, l^{[\bar{r}_n]}}^{[\bar{r}_n]} \right|$  bigger than that of the minimum non-zero element  $\left| \bar{\Gamma}_{k_n, l_n}^{(n)} \right|$ . Otherwise, the subcarrier allocation is not update, which means the end of the iteration in the proposed technique. Even in the following proposed techniques, if the subcarrier allocation matrix is not updated, the iteration is terminated.

The subcarrier allocation technique described in the section is called “Least Channel Gain Maximization With Channel Vector Swapping”, which is abbreviated as “CGVS”.

### B. Least LLR Maximization With Channel Vector Swapping

In the proposed techniques described above, the subcarrier allocation is searched for maximizing the least channel gain in the equivalent channel matrix. On the other hand, the MPA output signals can be used as better metric to select the

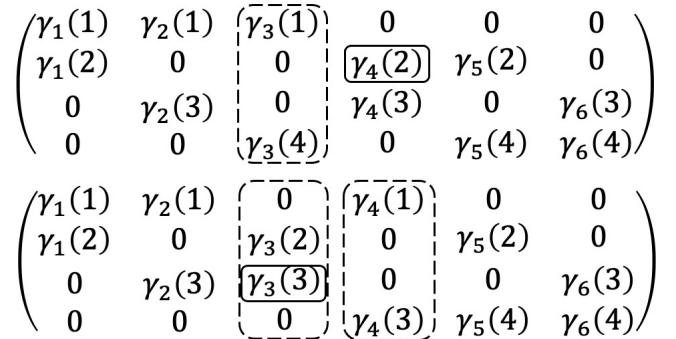


Fig. 1. Vector swapping in CGVS

<sup>1</sup>The number of the non-zero elements in the row vector of the subcarrier allocation matrix and that in the column vector correspond to that of the devices sending the packet in the subcarrier, and that of the subcarriers allocated to the device, respectively. Instead of non-zero element or column number, We explain the proposed technique with the terms of subcarriers and devices in this paragraph for readers to understand easily.

best permutation than the channel gains, because the MPA is employed at the receiver. In a word, it is better to use the MPA output signals for getting better subcarrier allocation matrix. As is done in the resource allocation with the vector swapping, firstly, the signal processing described in (12) and (13) is carried out to get the candidate subcarrier allocation matrix. With the matrix, the log-likelihood ratio is calculated in the following equation. Let  $\mathbf{X}^{(\beta)} \in \mathbb{C}^L$  denote a  $\beta$ th candidate of the transmission signal vector, a received signal at the  $k$ th subcarrier  $\dot{y}_{[r_n]}^{(\beta)}(k) \in \mathbb{C}$  in the non-orthogonal noise-free channel with the candidate subcarrier allocation matrix  $\mathbf{C}^{[r_n]}$  is written as,

$$\dot{y}_{[r_n]}^{(\beta)}(k) = \sum_{l=1}^L \bar{\mathbf{r}}_{k,l}^{[r_n]} x^{(\beta)}(l) = \bar{\mathbf{r}}_{\{k\}}^{[r_n]} \mathbf{X}^{(\beta)}. \quad (18)$$

In (18),  $x^{(\beta)}(l) \in \mathbb{C}$  represents an  $l$ th element of the vector  $\mathbf{X}^{(\beta)}$ , i.e.,  $\mathbf{X}^{(\beta)} = [x^{(\beta)}(1) \cdots x^{(\beta)}(L)]^T$ . The symbol LLR of the signal  $x^{(\beta)}(l)$  can be obtained as follows.

$$\begin{aligned} \Lambda_{[r_n],k}^{(\beta)}(x(l)=\alpha) &= \log \frac{P(x(l)=\alpha | \dot{y}_{[r_n]}^{(\beta)}(k))}{P(x(l)=\bar{\alpha} | \dot{y}_{[r_n]}^{(\beta)}(k))} \\ &\approx \max_{x(l)=\alpha} \left\{ -\frac{1}{2} |\dot{y}_{[r_n]}^{(\beta)}(k) - \bar{\mathbf{r}}_{\{k\}}^{[r_n]} \bar{\mathbf{X}}|^2 + \sum_{i \in B_{\{k\}}^{[r_n]} \setminus l} \frac{P(x(i))}{P(x(i)=\bar{\alpha})} \right\} \\ &\quad - \max_{x(l)=\bar{\alpha}} \left\{ -\frac{1}{2} |\dot{y}_{[r_n]}^{(\beta)}(k) - \bar{\mathbf{r}}_{\{k\}}^{[r_n]} \bar{\mathbf{X}}|^2 + \sum_{i \in B_{\{k\}}^{[r_n]} \setminus l} \frac{P(x(i))}{P(x(i)=\bar{\alpha})} \right\} \\ &\quad + \log \frac{P(x(l)=\alpha)}{P(x(l)=\bar{\alpha})} \end{aligned} \quad (19)$$

In (19),  $\Lambda_{[r_n],k}^{(\beta)}(x(l)=\alpha) \in \mathbb{R}$ ,  $P(a)$ ,  $P(Q|R)$ ,  $\bar{\mathbf{X}} \in \mathbb{C}^L$  and  $\bar{\alpha}$ , represent a symbol LLR of the modulation signal  $x(l)=\alpha$ , probability that an event  $a$  happens, conditional probability of an event  $Q$  when an event  $R$  occurred, a tentative transmission signal vector, and a reference modulation signal, respectively. In addition,  $B_{\{k\}}^{[r_n]}$  indicates a set containing positions of non-zero element in the row vector  $\bar{\mathbf{r}}_{\{k\}}^{[r_n]}$ , i.e.,  $B_{\{k\}}^{[r_n]} = \{l | \bar{\mathbf{r}}_{k,l}^{[r_n]} \neq 0\}$ . Let  $\alpha_{\max}$  denote a modulation signal that maximizes the LLR among all the modulation signal candidates except for the transmission signal  $x^{(\beta)}(l)$ , the reliability of the  $l$ th modulation signal  $\Delta\Lambda_{[r_n],k}^{(\beta)}(x(l)) \in \mathbb{R}$  is defined with the LLR as [14],

$$\begin{aligned} \Delta\Lambda_{[r_n],k}^{(\beta)}(x(l)) &= -\Lambda_{[r_n],k}^{(\beta)}(x(l)=\alpha_{\max}) \\ &\quad + \Lambda_{[r_n],k}^{(\beta)}(x(l)=x^{(\beta)}(l)) \end{aligned} \quad (20)$$

$\Delta\Lambda_{[r_n],k}^{(\beta)}(x(l)) \in \mathbb{R}$  can be regarded as reliability of the  $l$ th modulation signal in the  $k$ th subcarrier. Assuming that all the transmission signal vectors are generated with equal probability, the average reliability over all the subcarriers

TABLE I  
SIMULATION PARAMETERS

|  |                              |
|--|------------------------------|
| Modulation scheme                        | QPSK / OFDM                  |
| Number of DFT points                     | 128                          |
| Channel coding                           | Half rate convolutional code |
| Constraint length                        | 3                            |
| Decoding                                 | Viterbi algorithm            |
| Number of transmit antennas              | 1                            |
| Number of receive antennas               | 1                            |
| Number of subcarriers per device $M$     | 2                            |
| Number of IoT's devices                  | 6, 10, 15                    |
| Number of subcarriers per resource block | 4, 5, 6                      |
| Channel model                            | Multipath fading             |

can be defined as the reliability of the  $l$ th IoT device. The minimum reliability  $\gamma_n^{[r_n]} \in \mathbb{R}$  can be found as,

$$\gamma_n^{[r_n]} = \min_l \left[ \sum_{\beta} \sum_{k=0}^{N_s-1} \Delta\Lambda_{[r_n],k}^{(\beta)}(x(l)) \right]. \quad (21)$$

Since the IoT device index  $r_n$  ranges from 1 to  $L$ , the best IoT device index  $\bar{r}_n$  that maximizes the average reliability  $\Delta\Lambda_{[r_n],k}^{(\beta)}(x(l))$  is searched, and the best candidate subcarrier allocation matrix  $\mathbf{C}^{(n+1/n)}$  is obtained with the search result as follows.

$$\bar{r}_n = \arg \max_{r_n} [\gamma_n^{[r_n]}] \quad (22)$$

$$\mathbf{C}^{(n+1/n)} = \mathbf{C}^{(n)} \mathbf{J}(l_n \leftrightarrow \bar{r}_n) \quad (23)$$

As is done in the technique described above, the subcarrier allocation matrix  $\mathbf{C}^{(n)}$  is updated only if the swapping at this stage increases the smallest average reliability, which is written as,

$$\mathbf{C}^{(n+1)} = \begin{cases} \mathbf{C}^{(n+1/n)} & \gamma_{n-1}^{[\bar{r}_{n-1}]} < \gamma_n^{[\bar{r}_n]} \\ \mathbf{C}^{(n)} & \text{otherwise} \end{cases}. \quad (24)$$

The subcarrier allocation technique proposed in the section is called ‘‘Least LLR Maximization With Channel Vector Swapping (LLRVS)’’.

#### IV. COMPUTER SIMULATION

The performance of the frequency domain non-orthogonal multiple access based on the proposed subcarrier allocation is evaluated by computer simulation. The modulation scheme is quaternary phase shift keying (QPSK), and the half rate convolutional code with a constraint length of 3 is used. Multipath Rayleigh fading based on the Jakes’ model is applied to the channels between the base station and the devices. The number of the subcarriers  $N_F$  and that of the subcarriers allocated to one device  $M$  are 128 and 2, respectively. The resource block size  $N_s$  and the number of the devices  $L$  are set as  $(N_s, L) = (4, 6)$ ,  $(5, 10)$ , and  $(6, 15)$ , which correspond to the overloading ratios of 1.5, 2.0, and 2.5, respectively. Table I summarizes the simulation parameters. The performance of the fixed subcarrier allocation (FSA) is also evaluated as a reference, which is referred as the FSA in this paper.

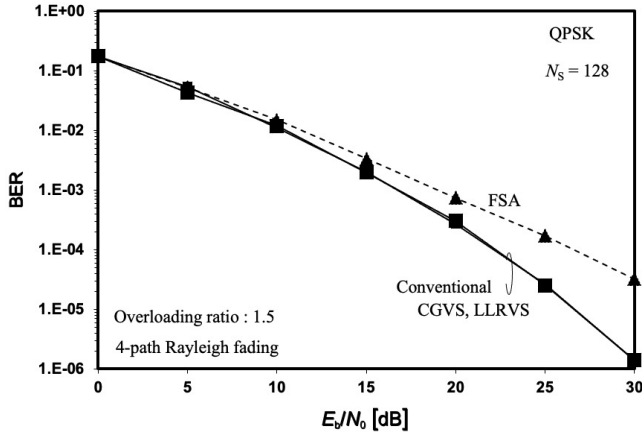


Fig. 2. BER performance (overloading ratio:1.5)

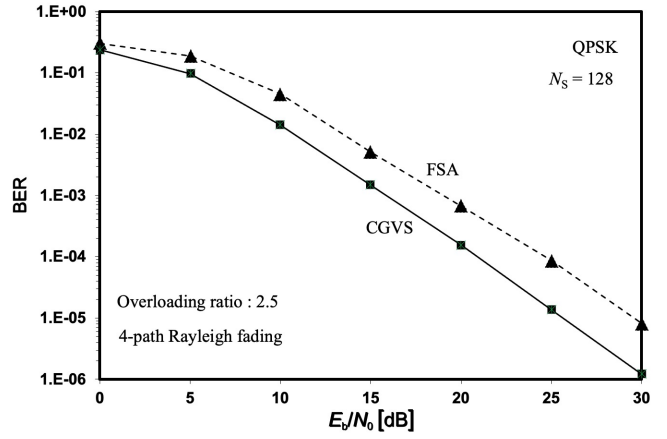


Fig. 4. BER performance (overloading ratio:2.5)

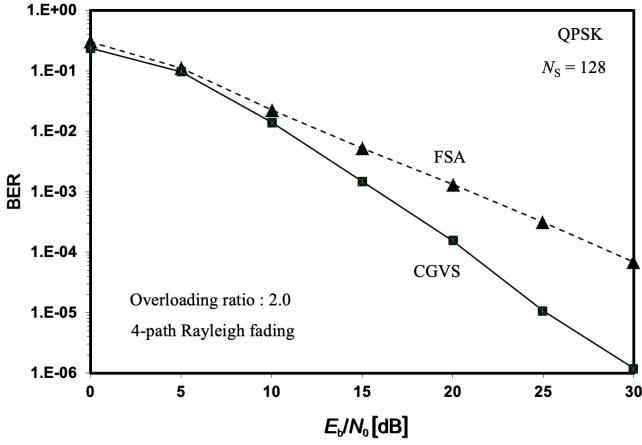


Fig. 3. BER performance (overloading ratio:2.0)

#### A. Comparison of Proposed Techniques

The proposed subcarrier allocation techniques are compared with each other in terms of the average bit error rate (BER) performance in Fig. 2. Horizontal axis is the  $E_b/N_0$  (dB). Overloading ratio is 1.5, i.e.,  $(N_s, L) = (4, 6)$ . 4 consecutive subcarriers are allocated to one resource block, which corresponds that  $b(k) = k_0 + k - 1$  where  $k_0$  represents an index of the subcarrier allocated to the first device. 4-path Rayleigh fading is applied to all the channels. In the figure, the performances of the FSA and the conventional technique are added as references<sup>2</sup>. The proposed CGVS and LLRVS achieve about 4dB better BER performance than the FSA at the BER of  $10^{-4}$ . They achieve the same performance to the conventional technique proposed in [14]. Fig. 3 shows the BER performance of the proposed techniques in the channel with the overloading ratio of 2.0, i.e.,  $(N_s, L) = (5, 10)$ .  $N_s$  consecutive subcarriers are allocated to one resource block. 4-path Rayleigh fading is applied. While the performance of the FSA is drawn as a reference, the performance of the

<sup>2</sup>The conventional technique has been proposed in [14], which is named as “MLR”. The MLR is shown to achieve the best performance among the techniques proposed in the literature.

conventional techniques can’t be obtained due to prohibitive high complexity, which will be shown in the following section. Fig. 4 shows the BER performance of the proposed techniques in the channel with the overloading ratio of 2.5, i.e.,  $(N_s, L) = (6, 16)$ . The channel model applied in Fig. 3 is also used. The performance of the FSA is added. The proposed techniques achieve similar performance even when the overloading ratio is increased from 1.5 to 2.5. Actually, CGVS and LLRVS attain a gain of about 10dB at the BER of  $10^{-4}$  when the overloading ratio is 2.0. When the overloading ratio is raised to 2.5, the gain is reduced to about 4dB at the BER of  $10^{-4}$ .

#### B. Complexity

The complexity of the proposed techniques are evaluated in terms of the number of multiplications. Fig. 5 shows the number of complex multiplications that is needed to get the subcarrier allocation matrix converged in the proposed techniques. Since the conventional technique executes the MPA for all the possible subcarrier allocation matrices generated by the vector swapping, the conventional technique has the highest complexity. On the other hand, LLRVS execute the MPA only if the vector is swapped. The LLRVS can be implemented with about  $10^{-5}$  smaller number of complex multiplications than the conventional technique, when the overloading ratio is 2.0. The complexity of CGVS is about  $10^{-16}$  as small as the conventional technique. Those complexity gap gets higher as the overloading ratio becomes bigger.

#### V. CONCLUSION

This paper has proposed low complexity subcarrier allocation for frequency domain non-orthogonal multiple access where many devices access with a base station. In the multiple access, a few subcarriers are allocated to each device, even if we assume that the number of the devices is more than that of the subcarriers a resource block. The proposed subcarrier allocation techniques adaptively search for subcarrier allocation that improves the transmission performance such as the average BER performance. This paper proposes 2 subcarrier

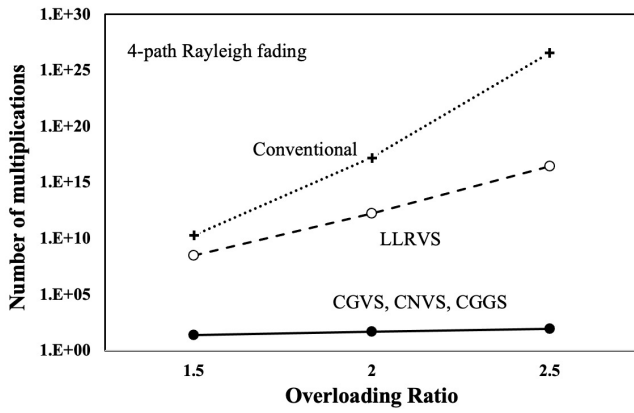


Fig. 5. Number of multiplications for precoding vector generation

allocation techniques, which are called “CGVS” and “LLRVS”. While they seek for better subcarrier allocation based on the MIN-MAX approach, the former technique searches nicer subcarrier allocation with only channel gains, which implements them with low computational complexity. The other technique applies the MPA to seek for better subcarrier allocation.

The proposed subcarrier allocation techniques are evaluated by computer simulation in frequency domain non-orthogonal multiple access. The proposed techniques achieve better transmission performance than the fixed subcarrier allocation in spite of the overloading ratio. In non-orthogonal multiple access with overloading ratio of 1.5, the “LLRVS” achieves the same performance to the conventional technique, which has been regarded as a technique to achieve the best performance. CGVS attains a gain of about 10dB at the BER of  $10^{-4}$  in the multiple access with the overloading ratio of 2.0.

The complexity of the proposed techniques are also evaluated by computer simulation in terms of the number of the complex multiplications. While LLRVS can be implemented with smaller complexity than the conventional technique, the complexity grows exponentially with the overloading ratio. On the other hand, the other proposed technique “CGVS” can be implemented with  $10^{-16}$  smaller complexity than the conventional technique when the overloading ratio is set to 2.0.

## VI. ACKNOWLEDGMENTS

This work was supported by JSPS KAKENHI Grant Number JP21K04061, support center for advanced telecommunications technology research (SCAT), and Softbank Corporation.

## REFERENCES

- [1] M. Ghosh, “A Comparison of Normalizations for ZF Precoded MU-MIMO Systems in Multipath Fading Channels,” *IEEE Wireless Commun. Letters*, Vol.2, No.5, pp.515-518, October 2013.
- [2] R. Aggarwal, M. Assaad, C. E. Koksal, and P. Schniter, “Joint Scheduling and Resource Allocation in the OFDMA Downlink: Utility Maximization Under Imperfect Channel-State Information,” *IEEE Trans. Signal Process.*, Vol.59, No.11, pp.5589-5604, November 2011.
- [3] A. Li, A. Benjebbour, X. Chen, H. Jiang, and H. Kayama, “Uplink Non-Orthogonal Multiple Access (NOMA) with Single-Carrier Frequency Division Multiple Access (SC-FDMA) for 5G Systems,” *IEICE Trans. Commun.*, Vol.E98-B, No.8, pp.1426-1435, August 2015.
- [4] A. Li, A. Benjebbour, K. Saito, Y. Kishiyama, and T. Nakamura, “Downlink Non-Orthogonal Multiple Access (NOMA) Combined with Single User MIMO (SU-MIMO),” *IEICE Trans. Commun.*, Vol.E98-B, No.8, pp.1415-1425, August 2015.
- [5] Q. Luo, P. Gao, Z. Liu, L. Xiao, Z. Mheich, P. Xiao, and A. Maaref, “An Error Rate Comparison of Power Domain Non-Orthogonal Multiple Access and Sparse Code Multiple Access,” *IEEE Open Journal of the Commun. Society*, Vol.2, pp.500-511, March 2021.
- [6] R. Stoica, G. Abreu, Z. Liu, T. Hara, and K. Ishibashi, “Massively Concurrent Non-Orthogonal Multiple Access for 5G Networks and Beyond,” *IEEE Access*, Vol.7, pp.82080-82100, June 2019.
- [7] S. M. A. Kazmi, N. H. Tran, T. M. Ho, D. Niyato, and C. S. Hong, “Coordinated Device-to-Device Communication With Non-Orthogonal Multiple Access in Future Wireless Cellular Networks,” *IEEE Access*, Vol.6, pp.39860-39875, June 2018.
- [8] K. Higuchi and A. Benjebbour, “Non-orthogonal Multiple Access (NOMA) with Successive Interference Cancellation for Future Radio Access,” *IEICE Trans. Commun.*, Vol.E98-B, No.3, pp.403-414, March 2015.
- [9] Q. Liu, Q. Zhang, X. Xin, R. Gao, Q. Tian, and F. Tian, “Subchannel and Power Allocation with Fairness Guaranteed for the Downlink of NOMA-Based Networks,” *IEICE Trans. Commun.*, Vol.E103-B, No.12, pp.1447-1461, December 2020.
- [10] R. Hoshyari, F. P. Wathan, and R. Tafazolli, “Novel low-density signature for synchronous CDMA systems over AWGN channel,” *IEEE Trans. Signal Process.*, Vol.56, No.4, pp.1616-1626, April 2008.
- [11] E. Okamoto and M. Hoshino, “Non-orthogonal Multiple Access Scheme Suitable for Machine Type Communication (MTC) and Its Applications,” *IEICE Trans. Commun.*, Vol.J100-B, No.8, pp.505-519, 2017.
- [12] V. H. Nikopour and H. Baligh, “Sparse code multiple access,” *Proc. IEEE Int’l Symp. Personal Indoor and Mobile Radio Communications (PIMRC)*, pp.332-336, September 2013.
- [13] X. Zhang, W. Ge, X. Wu, and W. Dai, “A Low-Complexity and Fast Convergence Message Passing Receiver Based on Partial Codeword Transmission for SCMA Systems,” *IEICE Trans. Commun.*, Vol.E101-B, No.11, pp.2259-2266, November 2018.
- [14] T. Yamagami, S. Denno, and Y. Hou, “Adaptive Resource Allocation Based on Factor Graphs in Non-Orthogonal Multiple Access,” *IEICE Trans. Commun.*, vol.E105-B, no.10, pp.-, 2022.
- [15] R. Gallager, “Low-density parity-check codes,” *IRE Trans. on Information Theory*, Vol.8-1, pp.21-28, January 1962.
- [16] R. Herzallah, “Probabilistic Message Passing for Decentralized Control of Stochastic Complex Systems,” *IEEE Access*, Vol.7, pp.184707-184717, December 2019.